We carried out a neurological examination and neuroradiological study in both patients and no comorbidities, including vascular disease, were seen, except for traumatic subarachnoid haemorrhage in patient 2.

### Pathological studies

Skeletal muscle samples were obtained from the biceps brachii. Serial frozen sections (8 μm) were prepared and stained with multiple histochemical methods (see online supplementary table 1).

Other sections prepared on aminosilane-coated slides were immunohistochemically stained with 1:50 diluted microtubule-associated protein 1 light chain 3B (LC-3) clone 5F10 (Nano Tools, France). Biotinylated anti-mouse IgG was used as the secondary antibody and the avidin–biotin–peroxidase complex (ABC) method was used for signal detection (ABC kit; Vector Laboratories, Burlingame, California, USA). All the immunohistochemical procedures were performed as reported previously.[7]

A small amount of the muscle specimens was fixed in glutaraldehyde in cacodylate buffer, post-fixed in 1% buffered osmium tetroxide and then embedded in Epon. Semi-thin sections were prepared for light microscopy to localise the target region, while ultra-thin sections were cut and stained with uranyl acetate and lead citrate for electron microscopy. The electron microscopy procedures were performed as described previously.[8]

### Mitochondrial DNA analysis

Genome DNA was extracted from both peripheral blood leucocytes (Qiagen, Maryland, USA) and frozen muscle specimens using a DNeasy blood and tissue kit (Qiagen). The entire mitochondrial DNA extracted from the skeletal muscles was sequenced using MitoChip V.2.0 (GeneChip Human Mitochondrial Resequencing Array 2.0) and analysed on GeneChip Sequence Analysis Software V4.0.[9 10] Previously described primers were used,[11] and the variations detected by MitoChip V.2.0 were then confirmed by direct Sanger sequencing, as described.[12]

The polymorphic and pathogenic natures of the confirmed mutations were checked against two databases: MITOMAP (http://www.mitomap.org/) and GiiB-JST mtSNP (http://mtsnp.tmig.or.jp/mtsnp/index.shtml).

### Heteroplasmic study

The GS Junior platform can sequence 1 00 000 single PCR fragments in parallel, which enables the detection of low levels of mtDNA heteroplasmy.[13 14] Using the Primer 3 program, we designed oligonucleotide primers flanking the m.8344A>G mutation (forward: 5′-CACTTTCACCGCTACACGAC-3′ and reverse: 5′-GCAATGAATGAAGCGAACAG-3′), which will generate a 428 bp PCR product. Using 50 ng genomic DNA from both blood and skeletal muscle of the two patients, after hot-start PCR, the products were sequenced on the GS Junior platform (Roche-454 Life Sciences, Basel, Switzerland) in accordance with the manufacturer's protocol. The results were assembled using the reference sequence (NC_012920) and analysed using GS Reference Mapper (454 Life Science) software.[15]

## RESULTS

### Pathological studies

In patients, histopathology showed moderate variation in muscle fibre size; numerous degenerating fibres with occasional regenerating or necrotic fibres were seen. RRFs were detected in 12.4% of muscle fibres (497/4001) in patient 1 and 20.7% of muscle fibres (253/1220) in patient 2. RVs were seen in occasional non-RRFs (figure 2). Cytochrome c oxidase activity was significantly decreased or absent in many fibres, particularly the RRFs, in which high succinate dehydrogenase expression was observed. The cytochrome c oxidase activity was increased in the non-RRF fibres containing isolated RVs. No blood vessels were seen that showed strong succinate dehydrogenase reactivity. Muscle fibres with RVs and RRFs, as well as some morphologically normal fibres, stained strongly for LC-3 (figure 3).

Electron microscopy in the biopsied muscle of the two patients disclosed significant abnormal mitochondrial proliferation with paracrystalline inclusions and circular arrangements of cristae. Autophagic vacuoles with membranous whorls and myelin-like structures were also seen (figure 4).

### Mitochondrial DNA analysis

Using MitoChip V.2.0, 57 mitochondrial DNA variations were detected in skeletal muscle samples from the two patients and 54 were confirmed to be single nucleotide polymorphisms (SNPs) by referring to the MITOMAP and GiiB-JST mtSNP databases. An m.8344A>G mutation in the $tRNA^{Lys}$ gene was detected in both patients and subsequently confirmed by direct sequencing of DNA from both muscle and blood lymphocytes (figure 5). In addition, a new SNP, m.306C>A in the non-coding area and a missense mutation m.3433T>A (Tyr43Asp) in the ND1 gene of patient 2 were also found. However, considering the vital role of the $tRNA^{Lys}$ gene, we considered m.8344A>G to be the causative mutation.

### Heteroplasmic study

Using the GS Junior platform, we clonally amplified and read more than 100 copies of each original amplicon from blood and muscle, in both patients. The percentage of 8344G in patient 1 was 17.8% (23/129) in blood and 45.1% (142/315) in muscle. In patient 2, the percentage was 25.2% (81/321) in blood and 80.3% (598/745) in muscle (figure 5).

## DISCUSSION

We selected five patients with suspected mitochondrial myopathy and characterised by the coexistence of RRFs and isolated RVs in muscle fibres. Using a resequencing microarray and a next-generation sequencing system, we identified both the m.8344A>G mutation and its heteroplasmic nature in two of these patients.

m.8344A>G, with a prevalence rate of no more than 0.25/100 000 in Europe, is the most common mutation of MERRF syndrome.[16–18] The clinical variations of MERRF syndrome are extensively expanded to encephalitis, infantile putaminal necrosis, depression, Parkinson's disease, cardiomyopathy, neuropathy, ophthalmoplegia, chronic pancreatitis and the MELAS phenotype that comprises mitochondrial encephalomyopathy, lactic acidosis and stroke-like episodes.[19–26] In our study, patient 1 had progressive proximal muscle weakness, restriction of superoinferior eye movement and hearing loss. Patient 2 experienced isolated skeletal muscle effects, with involvement of the facial and proximal upper limb muscles. Although they harboured the MERRF mutation, both patients presented with nearly isolated myopathy rather than the typical MERRF syndrome with myoclonus epilepsy or cerebellar ataxia.

RRFs formed the predominant pathological feature in 12.4% and 20.7% of fibres in patients 1 and 2, respectively. The combination of cytochrome c oxidase-negative fibres and abnormally proliferated mitochondria found in electron microscopy, confirmed the pathological diagnosis of mitochondrial myopathy. In both patients haematoxylin and eosin and mGT staining

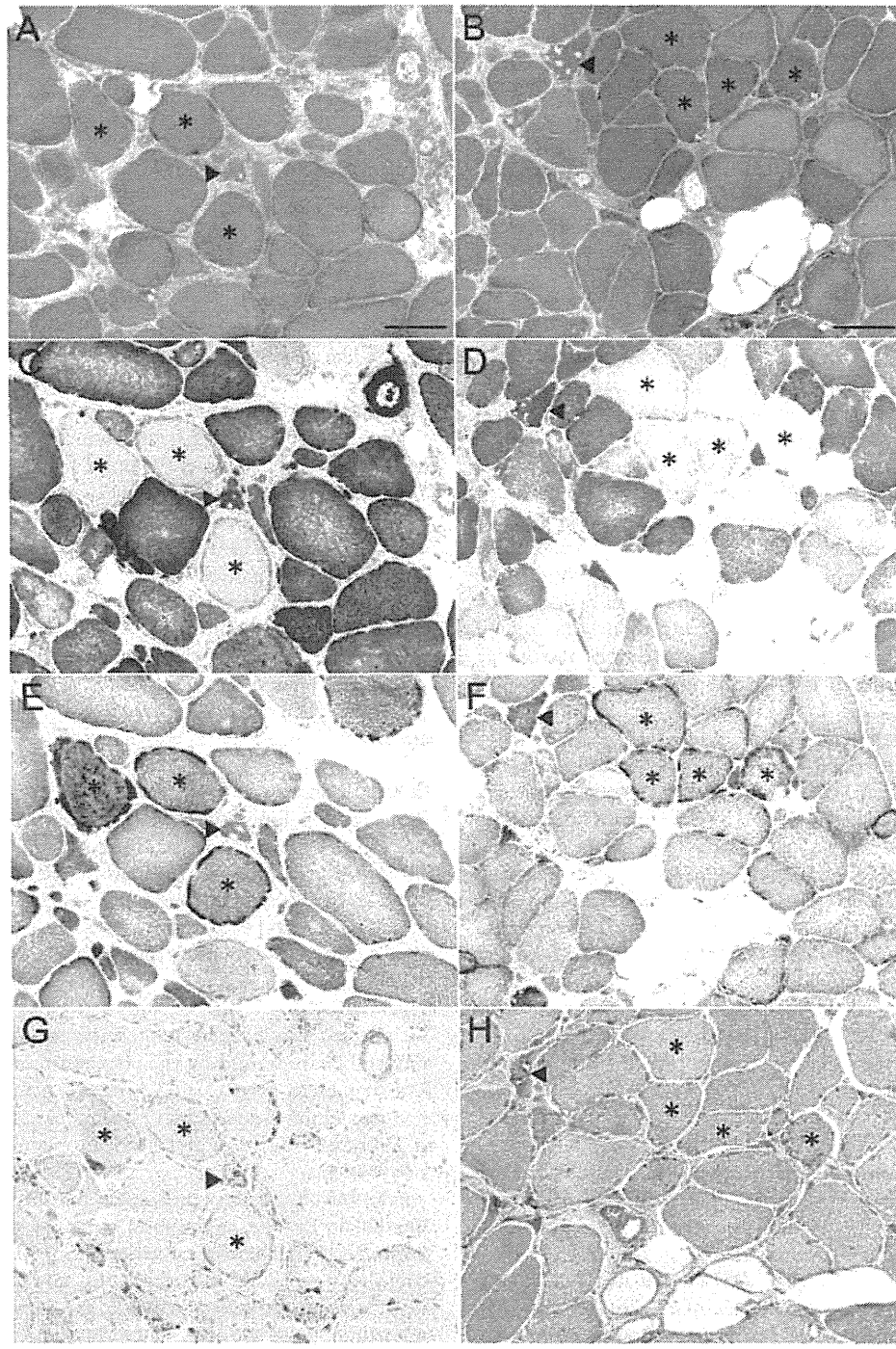


**Figure 3** Serial sections of histochemical and immunohistochemical stained skeletal muscle samples in patient 1 (A, C, E and G) and patient 2 (B, D, F and H). Moderate myopathic change with coexistence of numerous in muscle ragged-red fibres (RRFs) (*) and some rimmed vacuoles (▲) is seen with the modified Gomori trichrome stain (A and B). Cytochrome c oxidase activity is significantly decreased or absent in many fibres, particularly RRFs (C and D), with high succinate dehydrogenase expression (E and F). Immunohistochemical staining of LC-3 was strong in fibres with rimmed vacuoles and RRFs and also in some morphologically normal fibres (G and H). Bar=100 μm. Access the article online to view this figure in colour.

demonstrated RVs in fibres without mitochondrial accumulation or loss of cytochrome c oxidase activity. LC-3 aggregation was seen in fibres with isolated RVs, RRFs with secondary vacuolation and even in some fibres without any morphological changes. These abnormalities suggest the overexpression of autophagy or disorders of autophagic pathways in these fibres.[27] Electron microscopy also confirmed the existence of autophagic vacuoles. Although mild autophagic changes can be seen in RRFs of patients with common mitochondrial myopathies, conspicuous RVs and LC3-positive fibres in non-RRFs were the characteristic findings in both of our study patients. Additionally, degeneration, regeneration or necrosis of muscle fibres indicated active cellular damage, probably resulting from mitochondrial dysfunction.

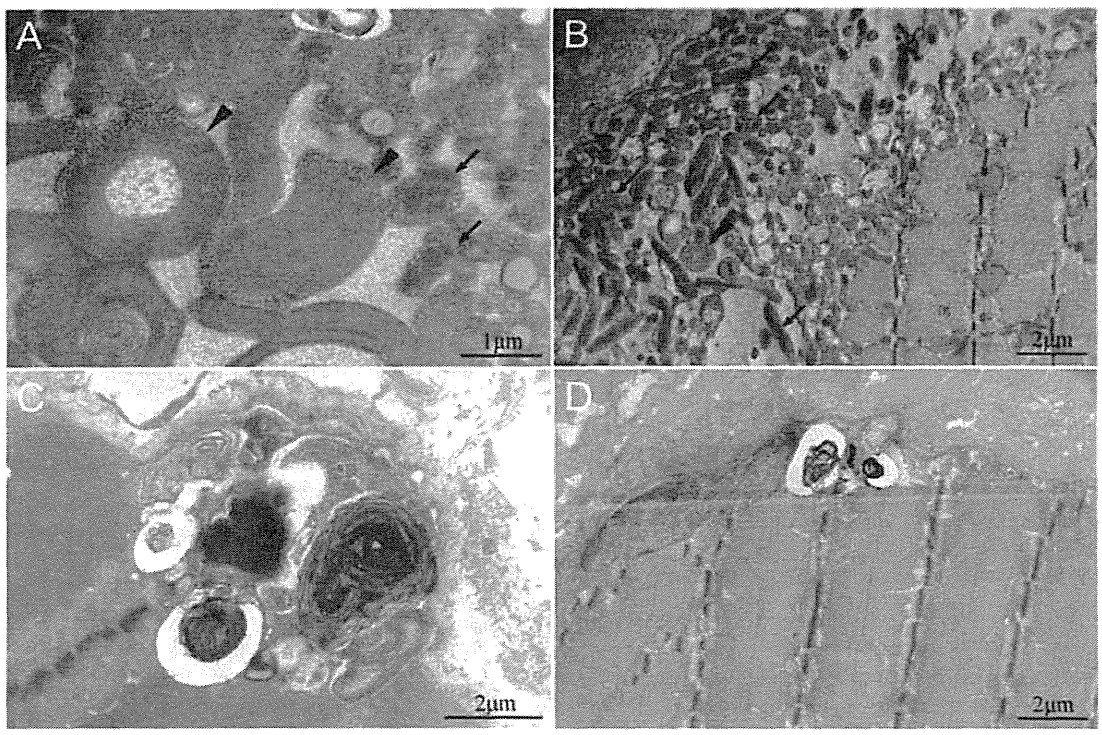


**Figure 4** Electron microscopy of abnormal mitochondria and autophagic vacuoles in skeletal muscle tissue from patient 1 (A and C) and patient 2 (B and D). Significant abnormal mitochondrial proliferation is seen, with paracrystalline inclusions (↙) and circular arrangements of cristae (▲) (A and B). Some autophagic vacuoles have membranous whorls and myelin-like structures (C and D). Access the article online to view this figure in colour.

It has been reported that the $tRNA^{Lys}$ gene with the m.8344A>G mutation particularly lacks post-transcriptional modification of uridine at the first letter of the anticodon (the wobble position)[28]; mutant tRNAs without the wobble modification cannot fulfil their normal role as acceptor molecules in the translation process, which results in respiratory chain defects and also in impaired global protein synthesis and compromised mitochondrial translation products.[29 30] Cells with the m.8344A>G mutation were recently shown to have increased autophagic activity.[31] We therefore postulate that the singular devastating effect of the m.8344A>G mutation in the $tRNA^{Lys}$ gene is to induce active autophagy for the purpose of abnormal mitochondria removal.

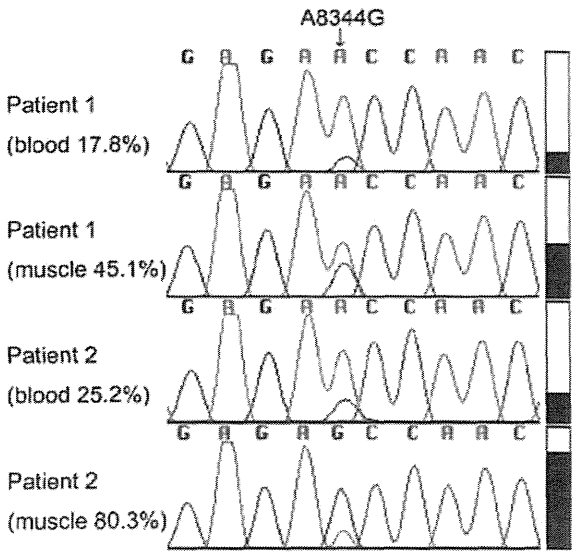


**Figure 5** Sequence chromatograms and block diagrams of m.8344A>G mutation heteroplasmy in both blood and skeletal muscle DNA from the two patients. The mutation rate in blood and skeletal muscle was 17.8% and 45.1% in patient 1, respectively, and 25.2% and 80.3%, respectively, in patient 2. The arrow indicates the mutation site. Access the article online to view this figure in colour.

Mutations in mtDNA including m.8344A>G are always heteroplasmic, meaning that mutant and wild-type genomes coexist. The autophagic targeting of mitochondria adds to this heterogeneity.[32] The threshold for biochemical expression of a mtDNA mutation varies, depending on the mutation and the tissue involved. In the muscle fibres containing isolated RVs, the heteroplasmy of mutated G may be below the threshold required to cause a RRF, but trigger the autophagy pathway first. The GS Junior platform was used to confirm the heteroplasmy of 8344G, and the relatively low heteroplasmy level in blood may explain the predominantly skeletal muscle phenotype seen in the two patients. We recommend that patients suspected of having a mitochondrial disorder undergo genetic analysis of mtDNA, using muscle as the preferred tissue type.

In summary, we focused on a rare pathological phenomenon of coexistence of RRFs and isolated RVs, and identified the m.8344A>G mutation in two patients with atypical MERRF syndrome. This finding suggests that the distinctive pathogenesis results from the m.8344A>G mutation in both patients. The autophagy, always considered to be a secondary process after mitochondrial dysfunction, may work earlier than expected. Although the mechanism of detailed interaction between the m.8344A>G mutation and autophagy requires further investigation, these findings broaden the pathological phenotype of patients with the m.8344A>G mutation.

## Take-home messages

- The interaction between autophagy and mitochondrial dysfunction remains unclear. The finding of isolated autophagic vacuoles in muscle fibres of patients with the m.8344A>G mutation, might be a starting point.
- The autophagic vacuoles, found in muscle fibres, might be associated with the atypical phenotype for a m.8344A>G mutation.
- The next-generation sequencing system might be reliable for detecting the heteroplasmy level of a mitochondrial DNA mutation.

**Acknowledgements** The authors thank N Hirata and Y Shirahama of our department for their excellent technical assistance. We also wish to thank the Joint Research Laboratory, Kagoshima University Graduate School of Medical and Dental Sciences for the use of their facilities.

**Contributors** J-HY carried out genetic experiments and drafted the manuscript. YS, YH and AY participated in genetic experiments and revised the manuscript. IH designed the study, revised the manuscript and obtained funding. YI, KH and AH carried out pathological and electron microscopy study. HT designed and supervised the study, revised the manuscript and obtained funding.

**Funding** The project was funded by the Ministry of Education, Culture, Sports, Science and Technology of Japan (grant 21591095 to HT; 21591094 to IH), intramural research grant (21B-1 to IH) for neurological and psychiatric disorders of the National Center of Neurology and Psychiatry, the Nervous and Mental Disorders and Research Committee for Charcot-Marie-Tooth disease, neuropathy, ataxic disease and applied health and technology of the Ministry of Health, Welfare and Labour, Japan and a research grant (23300201) from the Ministry of Health, Labour and Welfare of Japan.

**Competing interests** None.

**Ethics approval** Institutional review board of Kagoshima University.

**Provenance and peer review** Commissioned; externally peer reviewed.

## REFERENCES

1 Kumamoto T, Ueyama H, Tsumura H, *et al*. Expression of lysosome-related proteins and genes in the skeletal muscles of inclusion body myositis. *Acta Neuropathol* 2004;107:59–65.
2 Kim I, Rodriguez-Enriquez S, Lemasters JJ. Selective degradation of mitochondria by mitophagy. *Arch Biochem Biophys* 2007;462:245–53.
3 Geisler S, Holmström KM, Skujat D, *et al*. PINK1/Parkin-mediated mitophagy is dependent on VDAC1 and p62/SQSTM1. *Nat Cell Biol* 2010;12:119–31.
4 DiMauro S, Hirano M, Kaufmann P, *et al*. Clinical features and genetics of myoclonic epilepsy with ragged red fibers. *Adv Neurol* 2002;89:217–29.
5 Rifai Z, Welle S, Kamp C, *et al*. Ragged red fibers in normal aging and inflammatory myopathy. *Ann Neurol* 1995;37:24–9.
6 Shoffner JM, Lott MT, Lezza AM, *et al*. Myoclonic epilepsy and ragged-red fiber disease (MERRF) is associated with a mitochondrial DNA tRNA(Lys) mutation. *Cell* 1990;61:931–7.
7 Higuchi I, Niiyama T, Uchida Y, *et al*. Multiple episodes of thrombosis in a patient with Becker muscular dystrophy with marked expression of utrophin on the muscle cell membrane. *Acta Neuropathol* 1999;98:313–16.
8 Niiyama T, Higuchi I, Suehara M, *et al*. Electron microscopic abnormalities of skeletal muscle in patients with collagen VI deficiency in Ullrich's disease. *Acta Neuropathol* 2002;104:67–71.
9 Zhou S, Kassauei K, Cutler DJ, *et al*. An oligonucleotide microarray for high-throughput sequencing of the mitochondrial genome. *J Mol Diagn* 2006;8:476–82.
10 Mithani SK, Smith IM, Zhou S, *et al*. Mitochondrial resequencing arrays detect tumor-specific mutations in salivary rinses of patients with head and neck cancer. *Clin Cancer Res* 2007;13:7335–40.
11 Rieder MJ, Taylor SL, Tobe VO, *et al*. Automating the identification of DNA variations using quality-based fluorescence re-sequencing: analysis of the human mitochondrial genome. *Nucleic Acids Res* 1998;26:967–73.
12 Sakiyama Y, Okamoto Y, Higuchi I, *et al*. A new phenotype of mitochondrial disease characterized by familial late-onset predominant axial myopathy and encephalopathy. *Acta Neuropathol* 2011;121:775–83.
13 Li M, Schönberg A, Schaefer M, *et al*. Detecting heteroplasmy from high-throughput sequencing of complete human mitochondrial DNA genomes. *Am J Hum Genet* 2010;87:237–49.
14 Tang S, Huang T. Characterization of mitochondrial DNA heteroplasmy using a parallel sequencing system. *Biotechniques* 2010;48:287–96.
15 Holland MM, McQuillan MR, O'Hanlon KA. Second generation sequencing allows for mtDNA mixture deconvolution and high resolution detection of heteroplasmy. *Croat Med J* 2011;52:299–313.
16 Chinnery PF, Johnson MA, Wardell TM, *et al*. The epidemiology of pathogenic mitochondrial DNA mutations. *Ann Neurol* 2000;48:188–93.
17 Darin N, Oldfors A, Moslemi AR, *et al*. The incidence of mitochondrial encephalomyopathies in childhood: clinical features and morphological, biochemical and DNA abnormalities. *Ann Neurol* 2001;49:377–83.
18 Remes AM, Majamaa-Voltti K, Kärppä M, *et al*. Prevalence of large-scale mitochondrial DNA deletions in an adult Finnish population. *Neurology* 2005;64:976–81.
19 Orcesi S, Gorni K, Termine C, *et al*. Bilateral putaminal necrosis associated with the mitochondrial DNA A8344G myoclonus epilepsy with ragged red fibers (MERRF) mutation: an infantile case. *J Child Neurol* 2006;21:79–82.
20 Molnar MJ, Perenyi J, Siska E, *et al*. The typical MERRF (A8344G) mutation of the mitochondrial DNA associated with depressive mood disorders. *J Neurol* 2009;256:264–5.
21 Horvath R, Kley RA, Lochmuller H, *et al*. Parkinson syndrome, neuropathy and myopathy caused by the mutation A8344G (MERRF) in tRNALys. *Neurology* 2007;68:56–8.
22 Vallance HD, Jeven G, Wallace DC, *et al*. A case of sporadic infantile histiocytoid cardiomyopathy caused by the A8344G (MERRF) mitochondrial DNA mutation. *Pediatr Cardiol* 2004;25:538–40.
23 Erol I, Alehan F, Horvath R, *et al*. Demyelinating disease of central and peripheral nervous systems associated with a A8344G mutation in tRNALys. *Neuromuscul Disord* 2009;19:275–8.
24 Naini AB, Lu J, Kaufmann P, *et al*. Novel mitochondrial DNA ND5 mutation in a patient with clinical features of MELAS and MERRF. *Arch Neurol* 2005;62:473–6.
25 Nishigaki Y, Tadesse S, Bonilla E, *et al*. A novel mitochondrial tRNA(Leu(UUR)) mutation in a patient with features of MERRF and Kearns-Sayre syndrome. *Neuromuscul Disord* 2003;13:334–40.
26 Toyono M, Nakano K, Kiuchi M, *et al*. A case of MERRF associated with chronic pancreatitis. *Neuromuscul Disord* 2001;11:300–4.
27 Kuma A, Matsui M, Mizushima N. LC3, an autophagosome marker, can be incorporated into protein aggregates independent of autophagy: caution in the interpretation of LC3 localization. *Autophagy* 2007;3:323–8.
28 Yasukawa T, Suzuki T, Ishii N, *et al*. Defect in modification at the anticodon wobble nucleotide of mitochondrial tRNA(Lys) with the MERRF encephalomyopathy pathogenic mutation. *FEBS Lett* 2000;467:175–8.
29 Masucci JP, Schon EA, King MP. Point mutations in the mitochondrial tRNA(Lys) gene: implications for pathogenesis and mechanism. *Mol Cell Biochem* 1997;174:215–19.
30 Yasukawa T, Suzuki T, Ishii N, *et al*. Wobble modification defect in tRNA disturbs codon-anticodon interaction in a mitochondrial disease. *EMBO J* 2001;20:4794–802.
31 Chen CY, Chen HF, Gi SJ, *et al*. Decreased heat shock protein 27 expression and altered autophagy in human cells harboring A8344G mitochondrial DNA mutation. *Mitochondrion* 2011;11:739–49.
32 Wikstrom JD, Twig G, Shirihai OS. What can mitochondrial heterogeneity tell us about mitochondrial dynamics and autophagy? *Int J Biochem Cell Biol* 2009;41:1914–27.

Neurogenetics
DOI 10.1007/s10048-012-0313-1

ORIGINAL ARTICLE

# Vincristine exacerbates asymptomatic Charcot–Marie–Tooth disease with a novel *EGR2* mutation

**Tomonori Nakamura · Akihiro Hashiguchi · Shinsuke Suzuki · Kimiharu Uozumi · Shoko Tokunaga · Hiroshi Takashima**

Received: 1 November 2011 / Accepted: 9 January 2012


**Abstract** Neurotoxicity is a common side effect of vincristine (VCR) treatment. Severe exacerbations of neuropathy have been reported in patients with Charcot–Marie–Tooth disease (CMT) 1A with duplication of the *peripheral myelin protein 22* (*PMP22*) gene. However, whether or not VCR exacerbates neuropathies through mutations in other CMT-associated genes besides *PMP22* duplication has not been well studied. The purpose of this study was to identify mutations in any CMT-associated genes in a patient with hypersensitivity to VCR. We performed clinical, electrophysiological, and genetic examinations of a 23-year-old woman, who was hypersensitive to low-dose VCR, and her healthy mother. DNA analysis was performed using our specially designed resequencing array that simultaneously screens for 28 CMT-associated genes. Electrophysiological studies revealed that the patient and her healthy mother had demyelinating polyneuropathy. Furthermore, they showed the same novel mutation in the *early growth response 2* (*EGR2*) gene. Recognizing pre-existing asymptomatic CMT by electrophysiological studies and genetic analysis before VCR treatment allowed us to prevent severe VCR-induced neuropathy.

T. Nakamura · A. Hashiguchi · S. Tokunaga · H. Takashima (✉)
Department of Neurology and Geriatrics, Kagoshima University Graduate School of Medical and Dental Sciences,
Sakuragaoka 8-35-1,
Kagoshima City, Kagoshima 890-8520, Japan
e-mail: thiroshi@m3.kufm.kagoshima-u.ac.jp

S. Suzuki · K. Uozumi
Department of Hematology and Immunology, Kagoshima University Graduate School of Medical and Dental Sciences,
Sakuragaoka 8-35-1,
Kagoshima City, Kagoshima 890-8520, Japan

Published online: 25 January 2012

**Keywords** Charcot–Marie–Tooth disease · Early growth response 2 · Vincristine-induced neuropathy · DNA chip

## Introduction

Vincristine (VCR) is a vinca alkaloid drug that is an essential part of the chemotherapeutic regimens used to treat Hodgkin's and non-Hodgkin's lymphoma, acute lymphocytic leukemia, and several types of solid tumors. Neurotoxicity, the most frequently predominant distal axonal sensorimotor neuropathy, is a well-known dose-limiting side effect of VCR [1]. VCR disrupts microtubule functions in axons and inhibits axonal transport by binding and inactivating tubulin, thereby leading to axonal degeneration. VCR-induced neuropathy is usually observed after cumulative doses of 6–8 mg of VCR, and significant toxicity occurs at doses greater than 15–20 mg in neurologically normal individuals [2]. The symptoms of toxicity usually include paresthesia and muscle weakness in the distal extremities. Deep tendon reflexes often diminish or disappear. In most cases, neuropathy gradually improves as VCR is discontinued, but neuropathy can persist in some cases of severe sensorimotor dysfunction. Patients with pre-existing neuropathy are generally at increased risk of developing severe neuropathy after chemotherapy [2, 3]. Charcot–Marie–Tooth disease (CMT), a hereditary motor and sensory neuropathy, is one of the most common types of inherited neuropathies, with a prevalence rate of 1 in 2,500 [4], and it is clinically and genetically heterogeneous [5]. Until date, at least 30 genes are known to be associated with CMT and related inherited neuropathies (http://www.molgen.ua.ac.be/CMTMutations/Mutations). The most common type is CMT1A, which is an autosomal dominant demyelinating neuropathy associated with duplication of the *peripheral*

*myelin protein 22* (*PMP22*) gene. Some anticancer drugs such as vinca alkaloids, platinum agents, taxanes, and thalidomide are potentially toxic to patients with CMT [3, 6]. There are many reports of cases of CMT1A that deteriorated or were revealed after VCR treatment [7–12]. However, whether or not VCR exacerbates neuropathies in other types of CMT besides CMT1A is unclear. There is insufficient data to comment on the neurotoxicity of VCR in less common subtypes of CMT that affect other genes [13–15]. In order to identify the genetic risk of severe VCR-induced neuropathy, we screened for mutations in 28 CMT disease-causing genes using a custom resequencing DNA chip. Our DNA chip can screen 28 genes in 2 days and is relatively cost-effective. Using this chip, we identified a mutation in the *early growth response 2* (*EGR2*) gene in a 23-year-old woman with hypersensitivity to low-dose VCR. *EGR2* encodes a transcription factor that regulates the expression of peripheral myelin protein genes [16]. Although the risk of VCR-induced neuropathy in patients with an *EGR2* mutation is unknown, our high-throughput mutation screening method revealed a novel risk of developing drug-induced neuropathy.

## Materials and methods

### Patient

A 23-year-old woman was referred to our hospital with primary mediastinal large B-cell lymphoma. She presented no subjective clinical symptoms except mediastinal lymphadenopathies and was diagnosed with clinical stage IA (Ann Arbor Classification). At that time, she had not developed any neurological abnormalities. Her family seemed healthy and had no history of inherited or acquired neuropathies. She was treated with chemotherapy following the administration of rituximab, cyclophosphamide, doxorubicin, VCR, and prednisolone (day 1, 750 mg/m$^2$ cyclophosphamide, 50 mg/m$^2$ adriamycin, 1.4 mg/m$^2$ VCR; days 1–5, 100 mg prednisolone; and day 5, 375 mg/m$^2$ rituximab). After two courses (total VCR administered, 3.9 mg), she developed muscular weakness and paresthesia with pain in the distal extremities and was hardly able to walk. On day 49, she demonstrated distal predominant muscular weakness and paresthesia on neurological examination. No obvious muscular atrophy or pes cavus was evident. In addition, she had developed areflexia. Her Babinski reflex was negative, and there were no signs of cerebellar or cranial nerve disturbances.

### Electrophysiological studies

On day 54, nerve conduction studies were performed using the standard procedure. Skin temperature was maintained above 32°C.

### DNA analysis

Genomic DNA was extracted from the peripheral blood leukocytes of the patient using the Gentra Puregene Blood Kit (Qiagen, Tokyo, Japan). The purpose-built GeneChip® CustomSeq® Resequencing Array (Affymetrix, Santa Clara, CA) was designed to screen for CMT and related diseases such as ataxia with oculomotor apraxia type 1, ataxia with oculomotor apraxia type 2, spinocerebellar ataxia with axonal neuropathy type 1, and hereditary motor neuropathies. The resequencing array was designed to screen for the following 28 genes: *EGR2*, *PMP22*, *myelin protein zero* (*MPZ*), *gap junction protein beta 1* (*GJB1*), *periaxin* (*PRX*), *lipopolysaccharide-induced TNF factor* (*LITAF*), *neurofilament light polypeptide* (*NEFL*), *ganglioside-induced differentiation associated protein 1* (*GDAP1*), *myotubularin-related protein 2* (*MTMR2*), *SH3 domain and tetratricopeptide repeats 2* (*SH3TC2*), *SET-binding factor 2* (*SBF2*), *N-myc downstream regulated 1* (*NDRG1*), *mitofusin 2* (*MFN2*), *rab-protein 7* (*RAB7*), *glycyl-tRNA synthetase* (*GARS*), *heat shock 27 kDa protein 1* (*HSPB1*), *heat shock 22 kDa protein 8* (*HSPB8*), *lamin A/C* (*LMNA*), *dynamin 2* (*DNM2*), *tyrosyl-tRNA synthetase* (*YARS*), *alanyl-tRNA synthetase* (*AARS*), *lysyl-tRNA synthetase* (*KARS*), *aprataxin* (*APTX*), *senataxin* (*SETX*), *tyrosyl-DNA phosphodiesterase 1* (*TDP1*), *desert hedgehog* (*DHH*), *gigaxonin 1* (*GAN1*), and *K-Cl cotransporter family 3* (*KCC3*). We designed 363 primer sets to cover all the coding exons and splice sites. The 363 polymerase chain reactions (PCRs) were amplified in 32 multiplex reactions using the Qiagen Multiplex PCR system (Qiagen). Each reaction used 120 ng of genomic DNA, 10 pmol of the primer set, dNTP, and the Qiagen Multiplex PCR reaction mix (Qiagen). We generated each multiplex PCR product using the following conditions: 15 min at 95°C; 42 cycles of amplification (94°C for 30 s, 60°C for 3 min, and 72°C for 1 min 30 s); and 15 min at 68°C. Pooling, DNA fragmentation, labeling, and chip hybridization were performed using the Affymetrix CustomSeq Resequencing protocol instructions. The chips were washed using the Affymetrix fluidics station using the Customseq Resequencing wash protocols. Analysis of microarray data was performed using the GeneChip sequence Analysis Software version 4.0 (Affymetrix).

The mutations detected by our DNA chip method were confirmed by conventional DNA Sanger sequencing. Briefly, we amplified 50 ng of the patient's genomic DNA using primers and the hot start PCR method. Using a presequencing kit (USB, Cleveland, OH), we purified the patient's PCR products detected using our resequencing array method and sequenced them by dye–primer chemistry using an ABI Prism 377 Sequencer (Applied Biosystems, Foster City, CA). We then aligned the resulting sequences and evaluated the mutations using the Sequencher sequence alignment program (Gene Codes, Ann Arbor, MI).

## Results

### Electrophysiological studies

The motor nerve conduction studies revealed moderately slow motor nerve conduction velocities (MCV) with reduced compound muscle action potential (CMAP) amplitude in all examined nerves. The sensory nerve conduction studies showed moderately slow sensory nerve conduction velocities (SCV) with slightly reduced sensory nerve action potential (SNAP) amplitude (Table 1). No temporal dispersions or conduction blocks were observed. These results suggest demyelinating polyneuropathy complicated by axonal sensorimotor polyneuropathy. Because the patient showed hypersensitivity to low-dose VCR (total VCR administered, 3.9 mg), we suspected a pre-existing, inherited neuropathy. Furthermore, electrophysiological studies were performed on her healthy, 51-year-old mother. MCV of the mother was slower in the lower extremities than the upper extremities. CMAP amplitudes were within normal limits. Median nerve distal latency was slightly prolonged. SCV was moderately slow, but this finding was uniform in all examined nerves. SNAP amplitudes were moderately reduced in the upper extremities; SNAP amplitude of the sural nerve was at the lower limit of our normal control data. Temporal dispersions, conduction blocks, and entrapment neuropathies were not observed. These results indicate an electrophysiologically mild demyelinating polyneuropathy (Table 1). These findings suggest that this family may have an inherited demyelinating polyneuropathy.

### Resequencing analysis of this family and a control study

The DNA chip resequencing analysis detected a novel c.1057 C>G (p.R353G) missense mutation in the *EGR2* gene. In contrast, the analysis was negative for mutations involving the other 27 CMT or related disease-causing genes. The patient was heterozygous for the c.1057 C>G mutation that substitutes an arginine for glycine at amino acid 353 (p.R353G) in exon 2 of *EGR2* by conceptual translation (Fig. 1a). The mother had the same mutation as the patient (Fig. 1a). We did not observe R353G in 200 control chromosomes or in the 850 chromosomes from 425 patients with inherited neuropathy. In addition, we did not find the R353G mutation in the 1000 Genomes website (http://browser.1000genomes.org), which catalogs human genetic variations using 1,197 samples including 300 East Asian (100 Japanese) samples.

### Clinical course of the patient

We changed the chemotherapy regimen after we suspected that the patient had CMT. We chose radiotherapy and rituximab for the treatment of B-cell lymphoma. After 2 months, her symptoms had almost recovered, and she walked normally with only mild numbness in her distal lower limbs.

However, it was difficult to trace the causal agent because she was treated with a combination of chemotherapy agents. According to a previous report [3], there is uncertainty about the neurotoxicity of cyclophosphamide, prednisolone, and rituximab in patients with CMT, while VCR is classified as high risk for such patients. Furthermore, she and her mother's electrophysiological findings were consistent with inherited demyelinating polyneuropathy without the presence of conduction block or temporal dispersion. There were no findings indicated other inherited demyelinating polyneuropathy such as disturbance of lipid metabolism, peroxisomal disorders, hepatic porphyria and amyloidosis besides CMT. The results of her laboratory studies, including liver function tests, renal function tests, serum electrolyte and fasting blood glucose were normal. Her mother was healthy in the past periodic medical checkup, but laboratory

**Table 1** Results of the nerve conduction studies

| | Nerve | DL (ms) | CMAP amplitude (mV) | MCV (m/s) | SNAP amplitude (μV) | SCV (m/s) |
|---|---|---|---|---|---|---|
| Patient | Median | 4.3 | 1.5 | 26.9 | 6.7 | 45.1 |
| | Ulnar | 3.9 | 2.7 | 31.8 | 7.3 | 45.8 |
| | Tibial | 8.2 | 3.9 | 23.0 | – | – |
| | Sural | – | – | – | 4.2 | 33.3 |
| Patient's mother | Median | 5.0 | 11.2 | 44.6 | 3.9 | 39.7 |
| | Ulnar | 3.3 | 9.1 | 50.1 | 3.1 | 38.7 |
| | Tibial | 4.7 | 23.6 | 37.9 | – | – |
| | Sural | – | – | – | 5.2 | 37.6 |
| Control | Median | <4.5 | >3.1 | >49.6 | >7.0 | >47.2 |
| | Ulnar | <3.6 | >6.0 | >50.1 | >6.9 | >46.9 |
| | Tibial | <5.7 | >4.4 | >41.7 | – | – |
| | Sural | – | – | – | >5.0 | >40.8 |

*DL* distal latency, *CMAP* compound muscle action potential, *MCV* motor conduction velocity *SNAP* sensory nerve action potential, *SCV* sensory conduction velocity

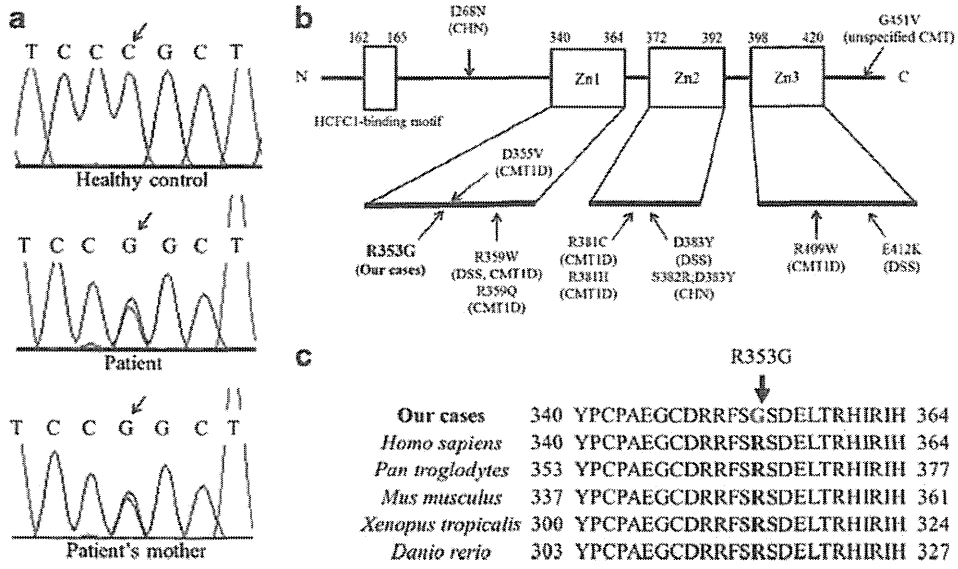


**Fig. 1** a Chromatograms of the alterations in the *early growth response 2* (*EGR2*) gene that was identified in the patient and her mother, both of whom had the heterozygous transition c.1057 C>G that resulted in R353G. b Schematic diagram of the *EGR2* showing previously reported mutations and the R353G alteration. *CHN* congenital hypomyelination neuropathy, *DSS* Dejerine–Sottas disease, *Zn* zinc-finger domains. c Comparison of *EGR2* mutations in different species

screening tests were not examined in this report. We strongly suspected VCR-induced neuropathy in CMT with the *EGR2* mutation.

## Discussion

This is the first report to describe an *EGR2* mutation that induced VCR hypersensitivity, similar to *PMP22* duplication. The *EGR2* gene located on human chromosome 10q21.1 has two exons that encode a 476 amino acid protein with three zinc finger domains, which is believed to be a transcription factor that regulates myelinogenesis [17, 18]. *EGR2* knockout mice exhibit severe hypomyelination of peripheral nerves due to the blocking of Schwann cell differentiation [19, 20]. Heterozygous mutations in *EGR2* cause myelinopathies, including congenital hypomyelinating neuropathy, Dejerine–Sottas disease, and mild to severe CMT1 [21–26]. Until date, 17 types of *EGR2* mutation have been found (http://www.molgen.ua.ac.be/CMTMutations/Mutations). *EGR2* induces high expression levels of myelin protein components such as *PMP22*, *MPZ*, *DHH*, and *PRX* in Schwann cells [27–30]. Vincristine inhibits axonal transport; thus, an insufficient supply of the myelin protein component necessary for the increased demand created by vincristine may induce a large degree of neurotoxicity. In the present study, we showed a novel R353G mutation in the first zinc finger domain of *EGR2* in a patient with late onset CMT1 who presented with

**Table 2** Computational predictions of the pathogenicity on EGR2 mutation within the zinc finger domain

| | Mutation | MUPro (SVM score[a]) | PolyPhen[b] | PolyPhen2[c] | SIFT[d] |
|---|---|---|---|---|---|
| Our patients | R353G | −0.43[e] | 2.57[e] | 0.90[e] | 0.00[e] |
| Reported mutations | D355V | 1.00 | 2.75[e] | 0.97[e] | 0.00[e] |
| | R359W | −0.64[e] | 2.79[e] | 1.00[e] | 0.00[e] |
| | R359Q | −1.00[e] | 1.89[e] | 0.92[e] | 0.00[e] |
| | R381C | −0.11[e] | 2.79[e] | 0.99[e] | 0.00[e] |
| | R381H | −0.24[e] | 2.12[e] | 0.99[e] | 0.00[e] |
| | S382R | 0.35 | 2.06[e] | 0.81[e] | 0.00[e] |
| | D383Y | 0.09 | 2.75[e] | 0.99[e] | 0.00[e] |
| | R409W | −0.98[e] | 2.69[e] | 1.00[e] | 0.00[e] |
| | E412K | −1.00[e] | 1.69[e] | 0.77[e] | 0.00[e] |

[a] Support Vector Machine (SVM) scores <0 indicate a decrease in protein stability

[b] PolyPhen scores ≥1.5 indicates a prediction of pathogenic

[c] PolyPhen2 scores of ~1 indicate a prediction of pathogenic

[d] SIFT scores ≤0.05 indicate a prediction of pathogenic

[e] Denotes a pathogenic prediction

a very mild phenotypic expression. Most *EGR2* mutations within the first zinc finger domain cause Dejerine–Sottas disease or severe CMT1 phenotypes (Fig. 1b) [22, 24]. A sequence homology search was performed, which aligned protein sequences from multiple species, using a Constraint-based, Multiple-Alignment tool (COBALT) (http://www.ncbi.nlm.nih.gov/tools/cobalt/). Arginine 353 was conserved among all of the species analyzed (Fig. 1c). It was found that the R353G mutation identified in our patients was located in a remarkably well-conserved sequence of amino acids, suggesting that it may have a potential impact on *EGR2* function. Furthermore, we computationally predicted the effect of the R353G mutation on protein function using the MUpro (http://www.ics.uci.edu/~baldig/mutation.html), PolyPhen (http://genetics.bwh.harvard.edu/pph/), PolyPhen-2 (http://genetics.bwh.harvard.edu/pph2/), and SIFT (http://sift.jcvi.org/www/SIFT_seq_submit2.html) algorithms. The algorithms in these programs use evolutionarily conserved species as well as reference sequence alignments, physiochemical differences, and the proximity of various substitutions to predict functional domains and/or structural features. All these programs predicted that the R353G mutation is most likely pathogen-based on the degree of conservation of the affected residues (Table 2). Therefore, the R353G mutation could possibly disrupt various functions. Furthermore, different mutations in the same codon result in divergent CMT phenotypes [26]. The electrophysiological findings were the only abnormal results for the patient's asymptomatic mother with the same *EGR2* mutation. Her neurological findings were normal, including a normal handgrip, the absence of foot deformities, normal and prompt deep tendon reflexes, and normal sensations. It is difficult to diagnose late onset mild CMT based on clinical findings and family history because the disease is heterogeneous. Although we did not perform in vitro functional analysis of the R353G mutation in this study, such further functional studies would illuminate the details of the pathomechanism of the *EGR2* mutation and its relationship with vincristine toxicity in this patient. In order to clarify the pathogenic nature of the *EGR2* mutation and vincristine neurotoxicity, we need to continue the genetic analysis of vincristine-induced neuropathy patients who do not show the CMT phenotype.

VCR-induced neuropathy is a dose-limiting side effect observed in neurologically normal individuals, but it sometimes results in severe neuropathy in patients with CMT. Early recognition of CMT before VCR treatment can prevent severe neurotoxicity. It is very important to use electrophysiological studies to recognize pre-existing CMT before VCR treatment, even if there is no family history or neurological abnormalities. Moreover, the labor and reagent costs of molecular genetic testing have significantly increased along with the increase in the number of genes associated with CMT and related neuropathies that must be screened for mutations. Realistically, it is difficult to perform nerve conduction studies or genetic testing in all patients who receive chemotherapy because of the costs and effort. Because of recent progress in the development of a new generation of genomic sequencing technologies, it will be possible to screen the entire genome/exome sequence for potential risks in all patients before they undergo chemotherapy.

**Acknowledgements** We thank the families described in this report for their cooperation. We also thank Ms. A. Yoshimura of Kagoshima University for her excellent technical assistance.

**Disclosures** This study was supported in part by grants from the Nervous and Mental Disorders and Research Committee for Charcot–Marie–Tooth Disease, Neuropathy, Ataxic Disease and Research on Applying Health Technology of the Japanese Ministry of Health, Welfare and Labor (H.T). H.T. has received royalty from Athena diagnostics.

## References

1. Weiss HD, Walker MD, Wiernik PH (1974) Neurotoxicity of commonly used antineoplastic agents (second of two parts). N Engl J Med 291:127–133
2. Trobaugh-Lotrario AD, Smith AA, Odom LF (2003) Vincristine neurotoxicity in the presence of hereditary neuropathy. Med Pediatr Oncol 40:39–43
3. Weimer LH, Podwall D (2006) Medication-induced exacerbation of neuropathy in Charcot–Marie–Tooth disease. J Neurol Sci 242:47–54
4. Birouk N, Gouider R, Le Guern E, Gugenheim M, Tardieu S, Maisonobe T, Le Forestier N, Agid Y, Brice A, Bouche P (1997) Charcot–Marie–Tooth disease type 1A with 17p11.2 duplication. Clinical and electrophysiological phenotype study and factors influencing disease severity in 119 cases. Brain 120:813–823
5. Boerkoel CF, Takashima H, Garcia CA, Olney RK, Johnson J, Berry K, Russo P, Kennedy S, Teebi AS, Scavina M, Williams LL, Mancias P, Butler IJ, Krajewski K, Shy M, Lupski JR (2002) Charcot–Marie–Tooth disease and related neuropathies: mutation distribution and genotype–phenotype correlation. Ann Neurol 51:190–201
6. Yerushalmi R, Levi I, Wygoda M, Ifergane G, Wirguin I (2007) Are platinum-based chemotherapeutic drugs safe for patients with Charcot–Marie–Tooth disease? J Peripher Nerv Syst 12:139–141
7. Neumann Y, Toren A, Rechavi G, Seifried B, Shoham NG, Mandel M, Kenet G, Sharon N, Sadeh M, Navon R (1996) Vincristine treatment triggering the expression of asymptomatic Charcot–Marie–Tooth disease. Med Pediatr Oncol 26:280–283
8. Mercuri E, Poulton J, Buck J, Broadbent V, Bamford M, Jungbluth H, Manzur AY, Muntoni F (1999) Vincristine treatment revealing asymptomatic hereditary motor sensory neuropathy type 1A. Arch Dis Child 81:442–443
9. Uno S, Katayama K, Dobashi N, Hirano A, Ogihara A, Yamazaki H, Usui N, Kobayashi T, Inoue K, Kuraishi Y (1999) Acute vincristine neurotoxicity in a non-Hodgkin's lymphoma patient with Charcot–Marie–Tooth disease. Rinsho Ketsueki 40:414–419
10. Hildebrandt G, Holler E, Woenkhaus M, Quarch G, Reichle A, Schalke B, Andreesen R (2000) Acute deterioration of Charcot–Marie–Tooth disease IA (CMT IA) following 2 mg of vincristine chemotherapy. Ann Oncol 11:743–747

11. Naumann R, Mohm J, Reuner U, Kroschinsky F, Rautenstrauss B, Ehninger G (2001) Early recognition of hereditary motor and sensory neuropathy type 1 can avoid life-threatening vincristine neurotoxicity. Br J Haematol 115:323–325
12. Cil T, Altintas A, Tamam Y, Battaloglu E, Isikdogan A (2009) Low dose vincristine-induced severe polyneuropathy in a Hodgkin lymphoma patient: a case report (vincristine-induced severe polyneuropathy). J Pediatr Hematol Oncol 31:787–789
13. Ajitsaria R, Reilly M, Anderson J (2008) Uneventful administration of vincristine in Charcot–Marie–Tooth disease type 1X. Pediatr Blood Cancer 50:874–876
14. Nishikawa T, Kawakami K, Kumamoto T, Tonooka S, Abe A, Hayasaka K, Okamoto Y, Kawano Y (2008) Severe neurotoxicities in a case of Charcot–Marie–Tooth disease type 2 caused by vincristine for acute lymphoblastic leukemia. J Pediatr Hematol Oncol 30:519–521
15. Porter CC, Carver AE, Albano EA (2009) Vincristine induced peripheral neuropathy potentiated by voriconazole in a patient with previously undiagnosed CMT1X. Pediatr Blood Cancer 52:298–300
16. Nagarajan R, Svaren J, Le N, Araki T, Watson M, Milbrandt J (2001) EGR2 mutations in inherited neuropathies dominant-negatively inhibit myelin gene expression. Neuron 30:355–368
17. Scherer SS (1997) The biology and pathobiology of Schwann cells. Curr Opin Neurol 10:386–397
18. Niemann A, Berger P, Suter U (2006) Pathomechanisms of mutant proteins in Charcot–Marie–Tooth disease. Neuromolecular Med 8:217–242
19. Swiatek PJ, Gridley T (1993) Perinatal lethality and defects in hindbrain development in mice homozygous for a targeted mutation of the zinc finger gene Krox20. Gene Dev 7:2071–2084
20. Topilko P, Schneider-Maunoury S, Levi G, Baron-Van Evercooren A, Chennoufi AB, Seitanidou T, Babinet C, Charnay P (1994) Krox-20 controls myelination in the peripheral nervous system. Nature 371:796–799
21. Warner LE, Mancias P, Butler IJ, McDonald CM, Keppen L, Koob KG, Lupski JR (1998) Mutations in the early growth response 2 (EGR2) gene are associated with hereditary myelinopathies. Nat Genet 18:382–384
22. Timmerman V, De Jonghe P, Ceuterick C, De Vriendt E, Lofgren A, Nelis E, Warner LE, Lupski JR, Martin JJ, Van Broeckhoven C (1999) Novel missense mutation in the early growth response 2 gene associated with Dejerine–Sottas syndrome phenotype. Neurology 52:1827–1832
23. Warner LE, Svaren J, Milbrandt J, Lupski JR (1999) Functional consequences of mutations in the early growth response 2 gene (EGR2) correlate with severity of human myelinopathies. Hum Mol Genet 8:1245–1251
24. Boerkoel C, Takashima H, Bacino C, Daentl D, Lupski J (2001) EGR2 mutation R359W causes a spectrum of Dejerine–Sottas neuropathy. Neurogenetics 3:153–157
25. Yoshihara T, Kanda F, Yamamoto M, Ishihara H, Misu K, Hattori N, Chihara K, Sobue G (2001) A novel missense mutation in the early growth response 2 gene associated with late-onset Charcot–Marie–Tooth disease type 1. J Neurol Sci 184:149–153
26. Mikesova E, Huhne K, Rautenstrauss B, Mazanec R, Barankova L, Vyhnalek M, Horacek O, Seeman P (2005) Novel EGR2 mutation R359Q is associated with CMT type 1 and progressive scoliosis. Neuromuscul Disord 15:764–767
27. Jang SW, LeBlanc SE, Roopra A, Wrabetz L, Svaren J (2006) In vivo detection of Egr2 binding to target genes during peripheral nerve myelination. J Neurochem 98:1678–1687
28. LeBlanc SE, Ward RM, Svaren J (2007) Neuropathy-associated Egr2 mutants disrupt cooperative activation of myelin protein zero by Egr2 and Sox10. Mol Cell Biol 27:3521–3529
29. Jang SW, Svaren J (2009) Induction of myelin protein zero by early growth response 2 through upstream and intragenic elements. J Biol Chem 284:20111–20120
30. Jones EA, Lopez-Anido C, Srinivasan R, Krueger C, Chang LW, Nagarajan R, Svaren J (2011) Regulation of the PMP22 gene through an intronic enhancer. J Neurosci 31:4242–4250

# Alanyl-tRNA synthetase mutation in a family with dominant distal hereditary motor neuropathy

Z. Zhao, MS
A. Hashiguchi, MD
J. Hu, MD, PhD
Y. Sakiyama, MD, PhD
Y. Okamoto, MD, PhD
S. Tokunaga, MD
L. Zhu, MB
H. Shen, MS
H. Takashima, MD, PhD

Correspondence & reprint requests to Dr. Hu: jinghujp@yahoo.com.cn

## ABSTRACT

**Objective:** To identify a new genetic cause of distal hereditary motor neuropathy (dHMN), which is also known as a variant of Charcot-Marie-Tooth disease (CMT), in a Chinese family.

**Methods:** We investigated a Chinese family with dHMN clinically, electrophysiologically, and genetically. We screened for the mutations of 28 CMT or related pathogenic genes using an originally designed microarray resequencing DNA chip.

**Results:** Investigation of the family history revealed an autosomal dominant transmission pattern. The clinical features of the family included mild weakness and wasting of the distal muscles of the lower limb and foot deformity, without clinical sensory involvement. Electrophysiologic studies revealed motor neuropathy. MRI of the lower limbs showed accentuated fatty infiltration of the gastrocnemius and vastus lateralis muscles. All 4 affected family members had a heterozygous missense mutation c.2677G>A (p.D893N) of alanyl-tRNA synthetase (*AARS*), which was not found in the 4 unaffected members and control subjects.

**Conclusion:** An *AARS* mutation caused dHMN in a Chinese family. *AARS* mutations result in not only a CMT phenotype but also a dHMN phenotype. **Neurology® 2012;78:1644–1649**

## GLOSSARY

**AARS** = alanyl-tRNA synthetase; **CMT** = Charcot-Marie-Tooth; **dHMN** = distal hereditary motor neuropathy; **MRC** = Medical Research Council; **SCV** = sensory nerve conduction velocity.

Distal hereditary motor neuropathy (dHMN) is also known as distal spinal muscular atrophy or a variant of Charcot-Marie-Tooth disease (CMT). dHMN is genetically and clinically heterogeneous. It has been classified into 7 subtypes according to age at onset, mode of inheritance, and the presence of additional features.[1] To date, at least 11 genes have been shown to be involved in dHMN: heat shock 27 kDa protein 1 (*HSPB1*), heat shock 22 kDa protein 8 (*HSPB8*), heat shock 27 kDa protein 3 (*HSPB3*), dynactin 1 (*DCTN1*), glycyl-tRNA synthetase (*GARS*), pleckstrin homology domain containing, family G (with RhoGef domain) member 5 (*PLEKHG5*), Berardinelli-Seip congenital lipodystrophy 2 (*BCSL2*), senataxin (*SETX*), immunoglobulin mu binding protein 2 (*IGHMBP2*), ATPase and $Cu^{2+}$ transporting, alpha polypeptide (*ATP7A*), and transient receptor potential cation channel, subfamily V, member 4 (*TRPV4*).[2] Interestingly, 5 of these genes (*HSPB8*, *HSPB1*, *GARS*, *TRPV4*, and *BCSL2*) have been described in CMT[2–6]; in some patients, dHMN and CMT phenotypes have been found to coexist.[7]

Four aminoacyl-tRNA synthetases (AARSs) have been implicated in CMT/dHMN:) glycyl (*GARS*; MIM 601472) in CMT2D and dHMN5A; 2) tyrosyl (*YARS*; MIM 608323) in dominant intermediate CMT type C; 3) alanyl (*AARS*; MIM 613287) in CMT2N; and 4) lysyl (*KARS*; MIM 601421) in CMT-recessive intermediate B and hereditary neuropathy with

From the Departments of Neuromuscular Disease (Z.Z., J.H., H.S.) and Electromyography (L.Z.), Third Hospital of Hebei Medical University, Shijiazhuang, PR China; and Department of Neurology and Geriatrics (A.H., Y.S., Y.O., S.T., H.T.), Kagoshima University Graduate School of Medical and Dental Sciences, Kagoshima, Japan.

*Study funding:* Supported in part by grants from the Nervous and Mental Disorders and Research Committee for Charcot-Marie-Tooth Disease, Neuropathy, Ataxic Disease and Practical Realization Research for Incurable Disease of the Japanese Ministry of Health, Welfare and Labor (H.T.).

Go to Neurology.org for full disclosures. Disclosures deemed relevant by the authors, if any, are provided at the end of this article.

liability to pressure palsies.[5,8–10] Although mutations in *AARS* cause axonal CMT, no published reports linking *AARS* mutations to the dHMN phenotype exist.

We report clinical and electrophysiologic findings in 3 patients with dHMN from a Chinese family carrying a novel missense mutation (D893N) in AARS.

## METHODS

We studied 3 generations of a Chinese family that included 4 affected and 8 unaffected members ascertained by neurologic examination (figure 1).

**Patients.** ***Patient 1.*** Patient 1 (III-1), now a 16-year-old boy, was referred to our neuromuscular disease department at the age of 11 years. He reported frequent falling and difficulty in rising from the squatting position since the age of 2 years; however, his condition had not deteriorated. Neurologic examination was initially performed at the first referral. His gait was almost normal, with no ataxia, but standing on his heels was difficult, and his heels could not touch the ground when squatting. Mild atrophy and weakness in the distal muscles of the lower limbs were observed, with a muscle strength score of 4 of 5 (Medical Research Council [MRC] scale) for the extensor digitorum brevis muscles, whereas the muscle strength scores of the iliopsoas, quadriceps femoris, biceps femoris, anterior tibial, and gastrocnemius muscles were 5 of 5 (MRC scale). However, the muscle strength of the quadriceps femoris and gastrocnemius muscles was relatively weaker than that of the iliopsoas or anterior tibial muscles. Pes cavus and toe clawing were noted (figure 2A). Sensory examination, including pain sensation, light touch sensation, position sensation, and vibration sensation of the 4 limbs was unremarkable. Deep tendon reflexes were decreased in the knees and absent in the ankles. Examination of the upper limbs was normal. There was no evidence of tremor or pyramidal tract signs.

***Patient 2.*** Patient 2 (I-2), the 67-year-old grandmother of the proband, first showed mild motor disability of the lower limbs at 55 years of age. Physical examination revealed distal motor weakness, wasting in the lower limbs, and pes cavus (figure 2B). Results of sensory examination including pain sensation, light touch sensation, position sensation, and vibration sensation of the 4 limbs were unremarkable. Deep tendon reflexes were absent in the lower limbs. Examination of the upper limbs was normal. There was no evidence of ataxia, tremor, or pyramidal tract signs.

***Patient 3 and patient 4.*** Neither patient 3 (II-1), the 44-year-old father, nor patient 4 (II-3), the 38-year-old aunt, of the proband experienced symptoms; however, neurologic examination revealed foot deformity, mild atrophy, and weakness of the lower limbs. The results of the sensory examination of patients 3 and 4 were similar to those of patients 1 and 2. Deep tendon reflexes were decreased in the knees and absent in the ankles.

**Standard protocol approvals, registrations, and patient consent.** The patients and family members included in this study gave written informed consent, and the study was approved by the Third Hospital of Hebei Medical University and the Institutional Review Board of Kagoshima University.

**Electrophysiologic study.** Needle EMG and nerve conduction velocity studies were performed in patients 1, 2, and 3.

**MRI study.** Skeletal muscle MRI of the lower limbs was performed in patient 1.

**Mutation screening.** Genomic DNA of 8 family members (I-1, I-2, II-1, II-2, II-3, II-5, III-1, and III-2) was extracted from the peripheral blood obtained using standard methods. The purpose-built GeneChip CustomSeq Resequencing Array (Affymetrix, Inc., Santa Clara, CA) was designed to screen for CMT and related diseases such as ataxia with oculomotor apraxia types 1 and 2, spinocerebellar ataxia with axonal neuropathy, and dHMN. We designed 363 primer sets to cover the entire coding regions and flanking sequences of the following 28 pathogenic genes: early growth response 2 (*EGR2*), peripheral myelin protein 22 (*PMP22*), myelin protein zero (*MPZ*), gap junction protein beta 1 (*GJB1*), periaxin (*PRX*), lipopolysaccharide-induced TNFα factor (*LITAF*), neurofilament light chain polypeptide (*NEFL*), ganglioside-induced differentiation-associated protein 1 (*GDAP1*), myotubularin-related protein 2 (*MTMR2*), SH3 domain and tetratricopeptide repeats 2 (*SH3TC2*), SET-binding factor 2 (*SBF2*), N-myc downstream regulated 1 (*NDRG1*), mitofusin 2 (*MFN2*), Ras-related GTPase 7 (*RAB7*), *GARS*, *HSPB1*, *HSPB8*, lamin A/C (*LMNA*), dynamin 2 (*DNM2*), *YARS*, *AARS*, *KARS*, aprataxin (*APTX*), senataxin (*SETX*), tyrosyl-DNA phosphodiesterase 1 (*TDP1*), desert hedgehog (*DHH*), gigaxonin 1 (*GAN1*), and K-Cl cotransporter 3 (*KCC3*) and 9 other candidate genes. The 363 PCR amplicons were amplified in 32 multiplex PCR reactions using the Qiagen Multiplex PCR system (Qiagen, Venlo, The Netherlands). Each reaction required 120 ng of genomic DNA, 10 pmol of primer sets, dNTP, and Qiagen Multiplex PCR Master Mix (Qiagen). The following conditions were used for multiplex PCR: 15 minutes at 95°C; 42 cycles of amplification (94°C for 30 s, 60°C for 3 minutes, and 72°C for 90 s); and 15 minutes at 68°C. Pooling, DNA fragmentation, labeling, and chip hybridization were performed according to the CustomSeq Resequencing protocol (Affymetrix, Inc.). Chips were washed using a Fluidics Station 450 (Affymetrix, Inc.) using CustomSeq Resequencing wash protocols. Analysis of microarray data was performed using GeneChip Sequence Analysis Software, version 4.0 (Affymetrix, Inc.).[11]

To confirm the mutation revealed by our DNA chip, the proband and 7 members of the family underwent genetic analy-

**Figure 1** **Pedigree of the distal hereditary motor neuropathy family**

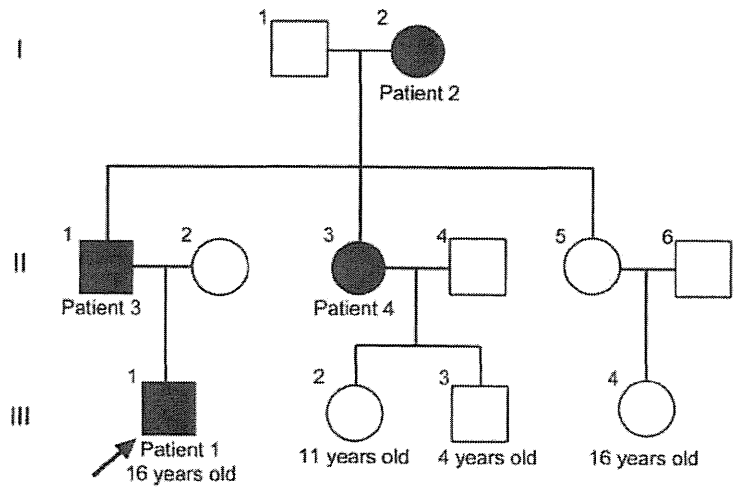


The arrow indicates the proband. Affected individuals are represented by solid black symbols; open symbols represent healthy individuals.

Figure 2 Clinical, radiologic, and genetic findings of the distal hereditary motor neuropathy family

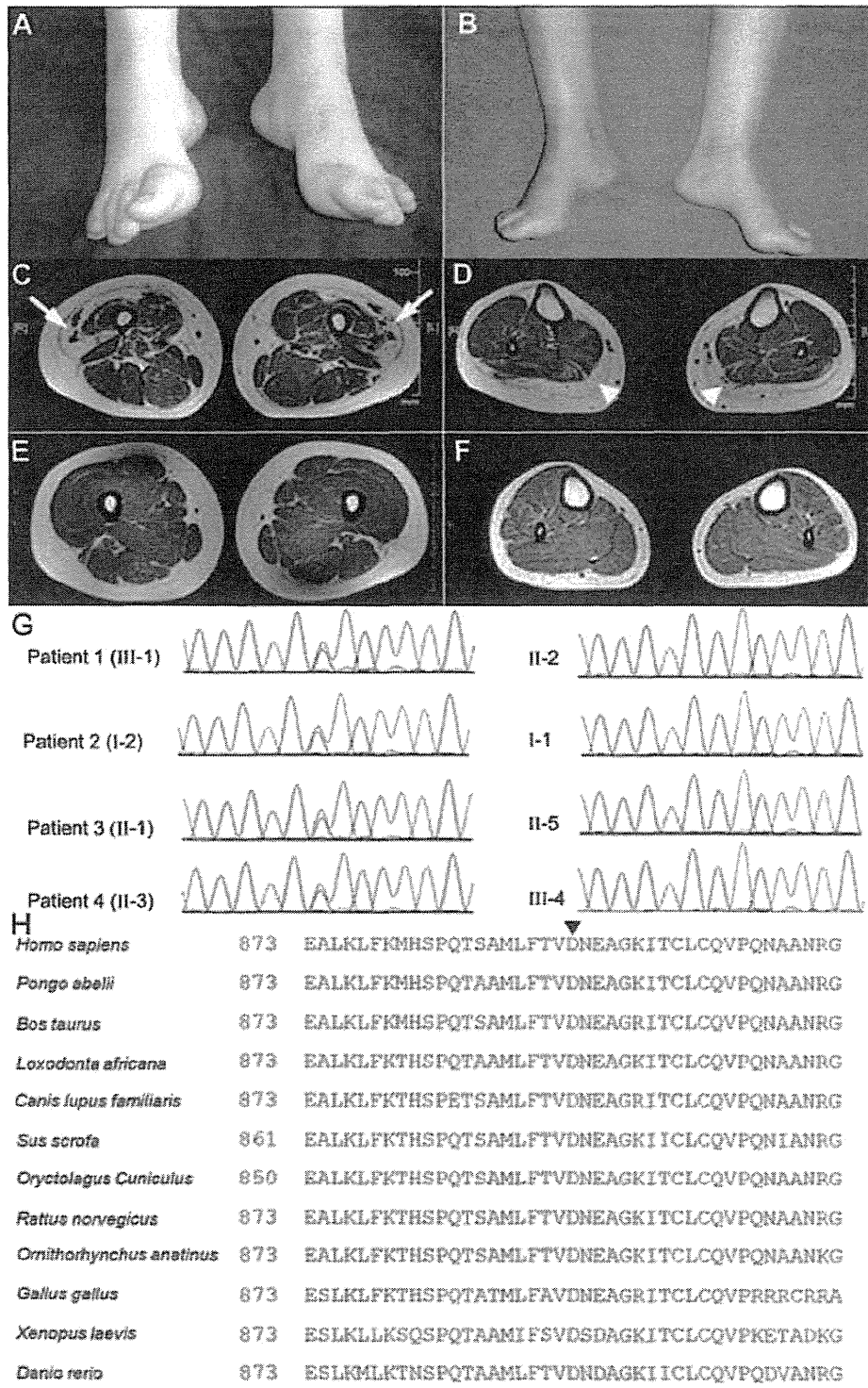


(A) A picture of patient 1 shows moderate pes cavus and toe clawing. (B) A picture of patient 2 shows pes cavus. (C and D) Axial T1-weighted images of the lower limbs in patient 1. (C) Axial image of the thighs, illustrating marked fatty replacement of the vastus lateralis muscle (arrows). (D) Axial image of the legs demonstrating complete fatty replacement of the gastrocnemius muscle (arrowheads). (E and F) Axial T1-weighted images of the lower limbs of a healthy control subject. (G) Chromatogram of the heterozygous c.2677G>A (p.D893N) mutation in exon 19 of *AARS*: left, 4 affected members; right, 4 unaffected relatives. (H) Comparison of AARS from different species. Arrowhead (▼) on top of the alignment indicates 893 amino acids.

Table Nerve conduction studies in patients 1, 2, and 3

| | Patient 1 | | | Patient 2 | | | Patient 3 | | |
|---|---|---|---|---|---|---|---|---|---|
| Nerve | MCV, m/s | DL, ms | CMAP, mV | MCV, m/s | DL, ms | CMAP, mV | MCV, m/s | DL, ms | CMAP, mV |
| Median | | | | | | | | | |
| E-W | 67 | | 11.2 | 57 | | 11.6 | 64 | | 21.8 |
| W-APB | | 2.6 | 11.2 | | 4.6[a] | 12.7 | | 2.6 | 22.0 |
| Ulnar | | | | | | | | | |
| E-W | 61 | | 4.1 | 60 | | 5.5 | 65 | | 10.4 |
| W-FI | | 2.5 | 4.3 | | 2.2 | 4.9 | | 2.1 | 10.6 |
| Peroneal | | | | | | | | | |
| K-A | 51 | | 4.7 | 48 | | 3.8 | 51 | | 10.1 |
| A-EDB | | 5.3 | 4.9 | | 3.1 | 4.0 | | 3.5 | 11.6 |
| | SCV, m/s | | SNAP, μV | SCV, m/s | | SNAP, μV | SCV, m/s | | SNAP, μV |
| Median | | | | | | | | | |
| IIIF-W | 54 | | 30 | 38[a] | | 13 | NE | | NE |
| Ulnar | | | | | | | | | |
| VF-W | 54 | | 12 | 54 | | 9 | NE | | NE |
| Sural | | | | | | | | | |
| A-sural | 48 | | 26 | 43 | | 28 | 56 | | 34 |

Abbreviations: A = ankle; APB = abductor pollicis brevis; CMAP = compound muscle action potential; DL = distal latency; E = elbow; EDB = extensor digitorum brevis; FI = first interossei; G = gastrocnemius; IIIF = third finger; K = knee; MCV = motor conduction velocity; PF = popliteal fossa; SCV = sensory conduction velocity; SNAP = sensory nerve action potential; VF = fifth finger; W = wrist.
[a] Abnormal value.

sis by direct sequencing. In brief, 50 ng of genomic DNA from the patients was amplified using the hot-start PCR method. Using a presequencing kit (USB Corp., Cleveland, OH), PCR products were purified and sequenced by dye terminator chemistry using an ABI Prism 377 DNA Sequencer (Applied Biosystems, Foster City, CA). The resulting sequences were then aligned, and mutations were evaluated using Sequencher version 4.8 sequence alignment software (Gene Codes, Ann Arbor, MI).

**RESULTS** **Electrophysiologic study.** Needle EMG revealed a neurogenic pattern, with a high frequency of large motor unit potentials recorded from the lower limbs of all 3 patients tested. Patient 1 showed normal sensory nerve conduction velocities (SCVs) and sensory nerve action potential of the median, ulnar, and sural nerves. Furthermore, he showed normal motor nerve conduction velocities and amplitudes of the compound muscle action potentials of the median, ulnar, and peroneal nerves. Patient 2 showed normal SCV, with a slight increase in distal latency in the median nerve and a mild decrease in SCV, suggestive of bilateral carpal tunnel syndrome. Patient 3 showed results similar to those of patient 1 (table). These findings indicate a chronic neurogenic pattern, suggesting that this family had inherited motor neuropathy.

**MRI study.** An axial T1-weighted MRI showed accentuated fatty infiltration of the gastrocnemius and vastus lateralis muscles (figure 2, C and D).

**Resequencing analysis and control study.** We identified one missense mutation, c.2677G>A (designated p.D893N), in exon 19 of *AARS*. All 4 family members considered to be clinically affected proved to have the heterozygous AARS p.D893N mutation, whereas none of the 4 unaffected relatives harbored this mutation (figure 2G). In addition, the mutation was not found in 220 East Asian (120 Chinese and 100 Japanese) control chromosomes or the chromosomes of patients with 850 inherited neuropathy nor did we find the D893N mutation in the 1000 Genomes Web site, which catalogs human genetic variations using 1,197 samples including 300 East Asian (200 Chinese) samples (http://browser.1000genomes.org).

**DISCUSSION** We report that an *AARS* mutation caused dHMN. A detailed investigation of the history of a family revealed 9 members over 3 generations, 4 of whom were affected individuals, consistent with a pattern of autosomal dominant transmission (figure 1). Clinical examination revealed benign wasting and weakness of the lower limbs. The diagnosis of dHMN was based on the history of autosomal dominant inheritance and electrophysiologic studies.

AARSs are a ubiquitously expressed, essential family of enzymes responsible for attaching amino acids to their cognate tRNAs in all cells and tissues. Mutations in 4 genes, *GARS*, *YARS*, *AARS*, and *KARS*, that encode AARSs have been implicated in CMT/dHMN.[5,8–10] Mutations in *GARS*, *YARS*, and *AARS* cause autosomal dominant CMT/dHMN. Two *KARS* mutations were detected in the compound heterozygous state in a patient with autosomal recessive CMT, developmental delay, self-abusive behavior, dysmorphic features, and vestibular schwannoma.[10] To elucidate the reason that mutations in ubiquitously expressed AARSs result in peripheral neuropathy, the effects of GARS, YARS, AARS, and KARS mutations in CMT/dHMN were investigated. A common pathologic mechanism for genetic disorders is a loss of gene function through altered mRNA or protein levels, although this is unusual for neurodegenerative diseases inherited in an autosomal dominant manner. Studies on G240R GARS heterozygous mutated lymphoblastoid cells did not reveal severely altered transcription, translation, or protein stability.[12] Pathogenic mechanisms such as defective aminoacylation, abnormal distribution in axons, or a combination of both are postulated to underlie CMT/dHMN, based on functional and protein localization studies of heterozygous GARS and AARS mutants.[9,12] Functional analyses of compound heterozygous mutations in *KARS* revealed severely affected enzyme activity.[10]

AARS catalyzes the attachment of alanine to its cognate tRNAs during protein synthesis. Investigation of the structure of AARS by X-ray crystallography revealed that it contains, from the N to the C terminus, an aminoacylation domain, a middle helical domain, an editing domain, and a so-called C-Ala domain.[13] The reported variant (R329H) is located in the middle helical domain, which together with the aminoacylation domain, is responsible for the complete and specific aminoacylation of AARS. The D893N variation is located in the C-Ala domain, which facilitates efficient editing by bringing together the aminoacylation and editing domains. A sequence homology search was performed to align protein sequences from multiple species, using a constraint-based multiple alignment tool (COBALT) (http://www.ncbi.nlm.nih.gov/tools/cobalt/). Aspartic acid 893 was conserved among all species analyzed (figure 2H). Thus, the D893N mutation identified in the Chinese dominant dHMN family is located in a remarkably well-conserved sequence of amino acids, suggesting that it may have a potential functional impact on AARS. Furthermore, we were able to computationally predict the effect of the D893N mutation on protein function using the MuPro (http://www.ics.uci.edu/~baldig/mutation.html) and PolyPhen-2 (http://genetics.bwh.harvard.edu/pph2/) algorithms, which gave scores of −0.334 and 0.802, respectively. MUPro scores of less than 0 indicate a decrease in protein stability, and PolyPhen-2 scores of approximately 1 indicate a prediction of pathogenicity. The D893N mutation is probably a pathogenic mutation, based on the degree of conservation of the affected residues.

Five genes (*HSPB8, HSPB1, GARS, TRPV4*, and *BCSL2*) have been described in both dHMN and CMT.[2–7] We add *AARS* on the basis of the present report. GARS and AARS are involved in common processes during protein synthesis, and the mutations reported to date were all missense mutations. Pathogenic missense mutations for autosomal dominant disease usually have a gain-of-function or dominant-negative effect. These pathogenic mutations of tRNA synthetases may directly disrupt protein synthesis.

Our data confirm that a mutation in the *AARS* gene (designated p.D893N) is associated with dominant dHMN in a Chinese family. This observation adds to a growing body of evidence that implicates specific genes/proteins in peripheral nerve function and delineates the pathologic consequences of their dysfunction.

## AUTHOR CONTRIBUTIONS

Z. Zhao and Dr. Hashiguchi contributed equally to this work. Dr. Hu and Dr. Takashima designed the research. Z. Zhao, Dr. Hashiguchi, Dr. Tokunaga, Dr. Sakiyama, and Dr. Okamoto performed genetic studies. L. Zhu, H. Shen, and Dr. Hu performed clinical research and provided patient information. Z. Zhao, Dr. Hu, and Dr. Takashima wrote the article.


## ACKNOWLEDGMENT

The authors thank the families described in this report for their cooperation and A. Yoshimura of Kagoshima University for her excellent technical assistance.


## DISCLOSURE

The authors report no disclosures relevant to the manuscript. **Go to Neurology.org for full disclosures.**


*Received October 18, 2011. Accepted in final form January 23, 2012.*


## REFERENCES


1. Harding AE. Inherited neuronal atrophy and degeneration predominantly of lower motor neurons. In: PJ Dyck, PK Thomas, eds. Peripheral Neuropathy. Philadelphia: WB Saunders; 1993.
2. Drew AP, Blair IP, Nicholson GA. Molecular genetics and mechanisms of disease in distal hereditary motor neuropathies: insights directing future genetic studies. Curr Mol Med 2011;11:650–665.
3. Irobi J, Van Impe K, Seeman P, et al. Hot-spot residue in small heat-shock protein 22 causes distal motor neuropathy. Nat Genet 2004;36:597–601.
4. Houlden H, Laura M, Wavrant-De Vrièze F, et al. Mutations in the HSP27 (HSPB1) gene cause dominant, reces-

sive, and sporadic distal HMN/CMT type 2. Neurology 2008;71:1660–1668.
5. Antonellis A, Ellsworth RE, Sambuughin N, et al. Glycyl tRNA synthetase mutations in Charcot-Marie-Tooth disease type 2D and distal spinal muscular atrophy type V. Am J Hum Genet 2003;72:1293–1299.
6. Windpassinger C, Auer-Grumbach M, Irobi J, et al. Heterozygous missense mutations in BSCL2 are associated with distal hereditary motor neuropathy and Silver syndrome. Nat Genet 2004;36:271–276.
7. Sambuughin N, Sivakumar K, Selenge B, et al. Autosomal dominant distal spinal muscular atrophy type V (dSMA-V) and Charcot-Marie-Tooth disease type 2D (CMT2D) segregate within a single large kindred and map to a refined region on chromosome 7p15. J Neurol Sci 1998;161:23–28.
8. Jordanova A, Irobi J, Thomas FP, et al. Disrupted function and axonal distribution of mutant tyrosyl-tRNA synthetase in dominant intermediate Charcot-Marie-Tooth neuropathy. Nat Genet 2006;38:197–202.
9. Latour P, Thauvin-Robinet C, Baudelet-Méry C, et al. A major determinant for binding and aminoacylation of $tRNA^{Ala}$ in cytoplasmic alanyl-tRNA synthetase is mutated in dominant axonal Charcot- Marie-Tooth disease. Am J Hum Genet 2010;86: 77–82.
10. McLaughlin HM, Sakaguchi R, Liu C, et al. Compound heterozygosity for loss-of-function lysyl-tRNA synthetase mutations in a patient with peripheral neuropathy. Am J Hum Genet 2010;87:560–566.
11. Cutler DJ, Zwick ME, Carrasquillo MM, et al. High-throughput variation detection and genotyping using microarrays. Genome Res 2001;11:1913–1925.
12. Antonellis A, Lee-Lin SQ, Wasterlain A, et al. Functional analyses of glycyl-tRNA synthetase mutations suggest a key role for tRNA-charging enzymes in peripheral axons. J Neurosci 2006;26:10397–10406.
13. Swairjo MA, Otero FJ, Yang XL, et al. Alanyl-tRNA synthetase crystal structure and design for acceptor-stem recognition. Mol Cell 2004;13:829–841.

J Neurol (2011) 258:1998–2008
DOI 10.1007/s00415-011-6056-3

ORIGINAL COMMUNICATION

# Nationwide survey of Alexander disease in Japan and proposed new guidelines for diagnosis

**Tomokatsu Yoshida · Masayuki Sasaki · Mari Yoshida · Michito Namekawa · Yuji Okamoto · Seiichi Tsujino · Hiroshi Sasayama · Ikuko Mizuta · Masanori Nakagawa · The Alexander Disease Study Group in Japan**

Received: 16 December 2010 / Revised: 10 April 2011 / Accepted: 11 April 2011 / Published online: 1 May 2011


**Abstract** Alexander disease (AxD) is a rare neurodegenerative disorder characterized by white matter degeneration and formation of cytoplasmic inclusions. *Glial fibrillary acidic protein* (*GFAP*) mutations have been reported in various forms of AxD since 2001. However, a definitive diagnosis remains difficult because of uncertain prevalence, and different clinical features seen in infantile AxD and adult AxD may lead to confusion and misdiagnosis. Here we report an epidemiological study conducted in Japan. Two nationwide questionnaire-based surveys were conducted using tentative diagnostic criteria. We gathered information regarding prevalence, neurological findings, magnetic resonance imaging (MRI) findings, electrophysiological findings, genetic information, and the results of therapeutic interventions and home care. Prevalence of various forms of AxD was determined as 27.3% (infantile), 24.2% (juvenile), and 48.5% (adult). Prevalence of AxD in Japan was estimated to be approximately 1 case per 2.7 million individuals. The main characteristics of infantile and juvenile AxD include delayed psychomotor development or mental retardation, convulsions, macrocephaly, and predominant cerebral white matter abnormalities in the frontal lobe on brain MRI. The main characteristics of adult AxD include bulbar signs, muscle weakness with hyperreflexia, and signal abnormalities and/or atrophy of medulla oblongata and cervical spinal cord on MRI. To ensure correct diagnosis of AxD, the physician should understand the importance of the process of *GFAP* genetic testing, which provides definitive diagnosis. Therefore, we propose new clinical guidelines for diagnosing AxD based on simplified classifications: cerebral AxD (type 1), bulbospinal AxD (type 2), and intermediate form (type 3).

**Keywords** Glial fibrillary acidic protein · Alexander disease · Genetics · Magnetic resonance imaging · Prevalence

**Abbreviations**

| | |
|---|---|
| AxD | Alexander disease |
| GFAP | Glial fibrillary acidic protein |
| EEG | Electroencephalogram |
| ABR | Auditory brainstem response |
| TRH | Thyroid-releasing hormone |

T. Yoshida (✉) · H. Sasayama · I. Mizuta · M. Nakagawa
Department of Neurology, Graduate School of Medical Science, Kyoto Prefectural University of Medicine, Kawaramachi Hirokoji, Kajii-chou 465, Kamigyo-ku, Kyoto 602-0841, Japan
e-mail: toyoshid@koto.kpu-m.ac.jp

M. Sasaki
Department of Child Neurology, National Center Hospital of Neurology and Psychiatry, Tokyo, Japan

M. Yoshida
Department of Neuropathology, Institute for Medical Science of Aging, Aichi Medical University, Aichi, Japan

M. Namekawa
Department of Neurology, Jichi Medical University, Tochigi, Japan

Y. Okamoto
Department of Neurology and Geriatrics, Kagoshima University Graduate School of Medicine and Dental Sciences, Kagoshima, Japan

S. Tsujino
Department of Rehabilitation, Osaka General Medical Center, Osaka, Japan

## Introduction

Alexander disease (AxD) is a rare neurodegenerative disorder characterized by white matter degeneration and formation of cytoplasmic inclusions known as Rosenthal fibers, which accumulate primarily in the astrocyte end-feet of subpial and perivascular zones and consist of glial fibrillary acidic protein (GFAP), heat shock protein 27, and αB-crystallin [1–3]. *Glial fibrillary acidic protein* mutations have been reported in various forms of AxD since 2001 [4]. AxD in adults was identified following research on various clinical forms of AxD and their associated findings detected by magnetic resonance imaging (MRI) [5]. Although adult AxD demonstrates a *GFAP* mutation, the clinical symptoms and MRI findings are different from those found in infantile AxD. Clinical features and MRI findings characteristic of AxD were recently identified by performing case studies and a systematic review [6–10]. However, a definitive diagnosis remains difficult because of uncertain prevalence; furthermore, different clinical features seen in infantile AxD and adult AxD may lead to confusion and misdiagnosis.

This study reports the results of a nationwide survey conducted in Japan to gather information on the prevalence, neurological findings, MRI findings, electrophysiological findings, genetic information, and the results of therapeutic interventions and home care.

## Materials and methods

Inclusion criteria specified for the diagnosis of AxD are summarized in Table 1. These criteria were decided on the basis of a literature review on AxD, and were decided for the three common age-dependent clinical subtypes, namely infantile, juvenile, and adult. MRI findings were based on previously reported proposed criteria [11].

### First survey

To determine the proportion of AxD patients in Japan, a survey questionnaire was sent to the members of educational facilities listed by the Japanese Societies of Neurology, Pediatrics, and Child Neurology, requesting information on patients who fulfilled the clinical inclusion criteria. Cases reported between 2004 and 2009 were examined in this survey.

### Second survey

A second set of survey questionnaires was mailed in November 2009 to facilities that were reported as having AxD patients in the first survey. Information was requested on patients' neurological, electrophysiological, and pathological findings, results of genetic analyses, treatment provided, and their clinical outcomes. We confirmed that these cases did not overlap with other reported cases by documenting age and place of birth.

Receipt of responses to the second survey was closed in February 2010, and the collected data were then analyzed.

The survey aimed at collecting information without many details, to obtain the maximum possible answers. Therefore, results were superficial, e.g., normal/abnormal, presence/absence of muscle weakness.

**Table 1** Requirements for the proposed diagnosis of Alexander disease for the first survey

Definite Alexander disease: existence of numerous Rosenthal fibers in addition to gliosis and loss of myelin in pathological study or *GFAP* gene mutation, and satisfaction of the following neurological and MRI findings 1, 2, or 3

1. Infantile Alexander disease: onset age is under 2 years with one or more items of (a) and one or more items of (b)

   (a) Neurological findings: psychomotor developmental delay/mental retardation, convulsion, macrocephaly spastic paralysis, bulbar or pseudobulbar signs, cerebellar ataxia

   (b) MRI findings: cerebral white matter abnormalities with frontal lobe predominance, signal abnormalities with swelling or atrophy of basal ganglia and thalami, periventricular rim, brainstem lesions, contrast enhancement

2. Juvenile Alexander disease: onset age is between 2 and 12 years with one or more items of (a) and one or more items of (b) (i) or (b) (ii)

   (a) Neurological findings: mental retardation or dementia, convulsion, macrocephaly spastic paralysis, bulbar or pseudobulbar signs, cerebellar ataxia, autonomic dysfunction, nystagmus, palatal myoclonus

   (b) MRI findings

   (i) Cerebral white matter abnormalities with frontal lobe predominance, signal abnormalities with swelling or atrophy of basal ganglia and thalami, periventricular rim, brainstem lesions, contrast enhancement

   (ii) Signal abnormalities or atrophy of medulla, oblongata, and/or cervical cord

3. Adult Alexander disease: onset age is over 12 years with one or more items of (a) and one or more items of (b)

   (a) Neurological findings: paralysis, bulbar or pseudobulbar signs, cerebellar ataxia, autonomic dysfunction, nystagmus, palatal myoclonus, dementia

   (b) MRI findings: signal abnormalities or atrophy of medulla oblongata and/or cervical cord

## Results

The results of the first and second surveys are summarized in Fig. 1.

Thirty-five patients with definite AxD were identified at the end of the surveys and were further analyzed. Prevalence of various forms of AxD was determined as infantile, 9/33 (27.3%); juvenile, 8/33 (24.2%); and adult, 16/33 (48.5%). Cases of twins with infantile AxD, and those with familial adult AxD were considered as one case; this was reflected in the calculations of the proportion of patients in each category.

Patient profiles are summarized in Table 2. Infantile AxD predominantly affected males (8 boys, 2 girls), while no gender predominance was observed in juvenile or adult AxD. Sixty-five percent of adult AxD patients had family members with AxD-like symptoms. Only one pair of identical twins presenting with similar clinical findings were diagnosed with infantile AxD, because brain biopsy of one of the twins showed characteristic Rosenthal fibers. In both cases, a *GFAP* mutation (R79C) was identified later.

Neurological findings are summarized in Table 3. Incidence of delayed psychomotor development or mental retardation, convulsions, macrocephaly, hyperreflexia, dysarthria, and dysphagia was high, whereas incidence of palatal tremor was zero in infantile AxD patients. Incidence of muscle weakness, hyperreflexia, dysarthria, dysphonia, dysphagia, and sphincter abnormalities was high in adult AxD patients. Three cases described as having "unilateral or asymmetric muscle weakness" were included. In addition, three cases that showed asymmetry in the initial stage of the disease, but not at the time of reporting, were also included. Asymmetry was identified in at least 35.0% of the adult AxD cases. Dementia and muscle rigidity were observed in 25.0% and 29.4% of adult AxD

Fig. 1 Flow of the survey

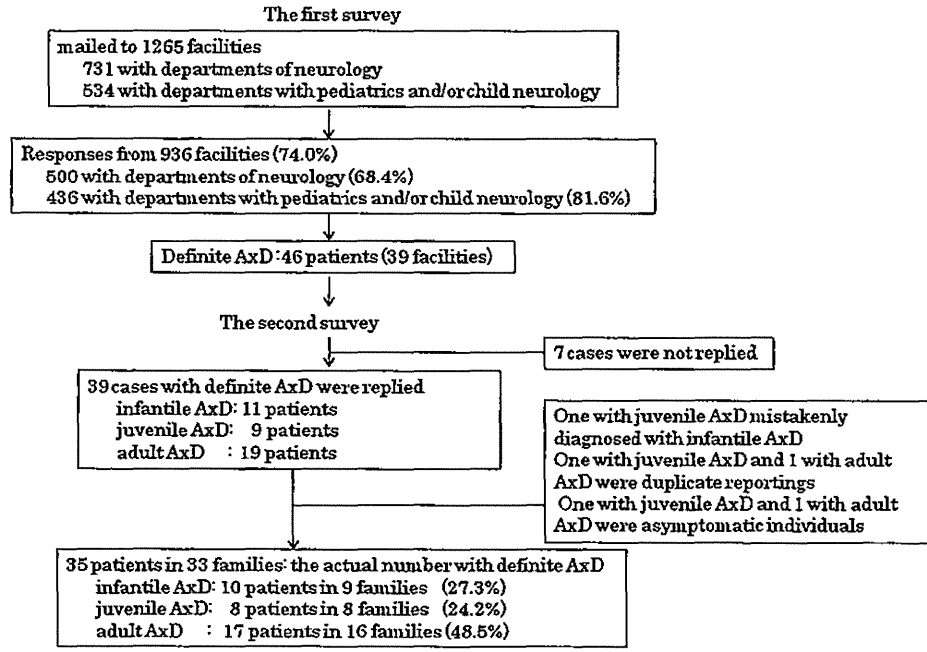


**Table 2** Patient profiles in the second survey

| | Infantile form | Juvenile form | Adult form |
|---|---|---|---|
| Cases | 10 | 8 | 17 |
| M:F | 8:2 | 4:4 | 9:8 |
| Age at onset (m: months, y: years) | 10.7 ± 6.7 m (3 to 24 m) | 4 0 ± 2.3 y (2 y 10 m to 9 y) | 44.1 ± 12.9 y (26 to 61 y) |
| Family history | 2 (twins) | 0 | 10 (9 families) |
| Period from onset to diagnosis | 60 ± 4 4 m (0 to 14 m) | 6.3 ± 3.1 y (<1 y 2 m to 10 y) | 6.9 ± 6.3 y (0 to 22 y) |
| *GFAP* gene analysis[a] | 10 | 8 | 17 |
| Pathological examination | 1 (brain biopsy) | 0 | 2 (autopsy) |

[a] *Glial fibrillary acidic protein* gene analysis was also preformed in two asymptomatic individuals

**Table 3** Summary of neurological signs of Alexander disease in the second survey

| | Infantile form | Juvenile form | Adult form |
|---|---|---|---|
| Muscle weakness | | 42.9% (3/7) | 82.4% (15/17) |
| Tender reflex abnormality | 85.7% (6/7) | 71.4% (5/7) | 94.1% (16/17) |
| Hyperreflexia | 85.7% (6/7) | 71.4% (5/7) | 94.1% (16/17) |
| Hyporeflexia or areflexia | | | 12.5% (2/16) |
| Babinski sign | | 57.1% (4/7) | 82.4% (14/17) |
| Parkinsonism | | 0.0% (0/7) | 29.4% (5/17) |
| Sensory disturbance | | 0.0% (0/7) | 17.6% (3/17) |
| Dysarthria | 100.0% (6/6) | 100.0% (8/8) | 88.2% (15/17) |
| Dysphonia | 66.7% (6/9) | 37.5% (3/8) | 70.6% (12/17) |
| Dysphagia | 77.8% (7/9) | 25.0% (2/8) | 88.2% (15/17) |
| Nystagmus | 0.0% (0/6) | 0.0% (0/8) | 64.7% (11/17) |
| Limb ataxia | 20.0% (1/5) | 37.5% (3/8) | 30.8% (4/13) |
| Truncal ataxia | 20.0% (1/5) | 50.0% (4/8) | 50.0% (6/12) |
| Palatal myoclonus | 0.0% (0/6) | 0.0% (0/7) | 37.5% (6/16) |
| Orthostatic hypotension | | 20.0% (1/5) | 7.7% (1/13) |
| Sphincter abnormalities | 33.3% (3/9) | 12.5% (1/8) | 57.1% (8/14) |
| Sleep disorder | | 25.0% (1/4) | 30.8% (4/13) |
| Convulsions | 100.0% (9/9) | 87.5% (7/8) | 6.3% (1/16) |
| Mental retardation/psychomotor developmental delay | 100.0% (8/8) | 87.5% (7/8) | 6.3% (1/16) |
| Dementia | | | 25.0% (4/16) |
| Macrocephaly | 75.0% (6/8) | 50.0% (4/5) | |
| Scoliosis | 44.4% (4/9) | 50.0% (4/8) | 13.3% (2/15) |

**Table 4** Summary of MRI findings of Alexander disease in the second survey

| | Infantile form | Juvenile form | Adult form |
|---|---|---|---|
| White matter lesion | 100% (10/10) | 100% (8/8) | 37.5% (6/16) |
| Abnormalities of basal ganglia, thalamus | 100% (9/9) | 50.0% (4/8) | 50.0% (8/16) |
| Abnormalities of brainstem | | | |
| Medulla oblongata | 14.3% (1/7) | 62.5% (5/8) | 100% (16/16) |
| Pons | 14.3% (1/7) | 62.5% (5/8) | 75.0% (12/16) |
| Midbrain | 28.6% (2/7) | 57.1% (4/7) | 75.0% (12/16) |
| Abnormalities of cervical cord | 25.0% (1/4) | 20.0% (1/5) | 100% (16/16) |
| Abnormalities of cerebellum | 37.5% (3/8) | 50.0% (4/8) | 62.5% (10/16) |
| Periventricular rim | 100% (7/7) | 62.5% (5/8) | 31.3% (5/16) |
| Enhancement | 75.0% (3/4) | 50.0% (1/2) | 8.3% (1/12) |

patients, respectively. Three cases with clinical findings similar to frontotemporal dementia were mentioned in the free comments section of the questionnaire. Sleep disorders, such as sleep apnea syndrome or rapid eye movement (REM) sleep behavior disorder, and palatal tremor were observed in 30.8% and 37.5% of the adult AxD patients, respectively. Incidence of dysarthria, convulsions, mental retardation, and hyperreflexia was high in juvenile AxD patients.

MRI findings are summarized in Table 4. Cerebral white matter abnormalities in the frontal lobe, signal abnormalities indicating swelling or atrophy of the basal ganglia and thalami, and periventricular rim of low signal intensity on T2-weighted images and high signal intensity on T1-weighted images were predominantly observed in all infantile AxD patients, whereas brainstem lesions were present in only a small number of these patients. Medulla oblongata and cervical spinal cord abnormalities were observed in all adult AxD patients, while abnormalities of other structures related to the brainstem and cerebellum were observed in 60–70% of adult AxD patients. Furthermore, abnormal signals of nucleus dentatus and middle cerebellar peduncle were observed in a few cases reported in the free comments section of the second survey form.